

Present-day crustal deformation around Sagaing fault, Myanmar

Christophe Vigny,¹ Anne Socquet,¹ Claude Rangin,¹ Nicolas Chamot-Rooke,¹ Manuel Pubellier,¹ Marie-Noëlle Bouin,² Guillaume Bertrand,^{1,3} and M. Becker⁴

Received 29 May 2002; revised 7 July 2003; accepted 23 July 2003; published 19 November 2003.

[1] Global Positioning System (GPS) measurement campaigns in Myanmar, conducted in 1998 and 2000, allow quantifying the present-day crustal deformation around the Sagaing fault system in central Myanmar. Both a regional network installed at four points within the country and a local 18-station network centered on the city of Mandalay across the Sagaing fault demonstrate that active deformation related to the northward motion of India is distributed across Myanmar in a platelet that extends from the western edge of the Shan Plateau in the east to the Andaman Trench in the west. In this platelet, deformation is rather diffuse and distributed over distinct fault systems. In the east, the Sagaing/Shan Scarp fault system absorbs <20 mm/yr of the 35 mm/yr India/Sundaland strike-slip motion. Along this major plate boundary, strain is partitioned along the N-S trending Sagaing fault and the transtensive N160°E trending Shan Scarp fault. Shortening and wrenching within the inverted central Myanmar basins, strike-slip faults affecting the Arakan Yoma fold-and-thrust belt, and oblique subduction along the Andaman trench should absorb the remaining India/Sundaland motion (>10 mm/yr). This GPS study combined with an on land geotectonic survey demonstrate that oblique slip of India along the rigid Sundaland block is accommodated by a partitioned system characterized by distribution of deformation over a wide zone. *INDEX TERMS*: 1206 Geodesy and Gravity:

Crustal movements—interplate (8155); 1243 Geodesy and Gravity: Space geodetic surveys; 8110

Tectonophysics: Continental tectonics—general (0905); 8158 Tectonophysics: Plate motions—present and recent (3040); *KEYWORDS*: tectonics, GPS, fault, Southeast Asia

Citation: Vigny, C., A. Socquet, C. Rangin, N. Chamot-Rooke, M. Pubellier, M.-N. Bouin, G. Bertrand, and M. Becker, Present-day crustal deformation around Sagaing fault, Myanmar, *J. Geophys. Res.*, 108(B11), 2533, doi:10.1029/2002JB001999, 2003.

1. Introduction

[2] The global plate motion model NNR-NUVEL-1A [DeMets *et al.*, 1994] predicts a relative motion of India with respect to Eurasia of ~54 mm/yr oriented around N20°E on the eastern border of the Indian plate in Myanmar. Taking into account a more recent, and somewhat slower, geodetic determination of the Indian motion, one obtains a reduced motion rate of ~47 mm/yr oriented roughly in the same direction (around 23°) [Paul *et al.*, 2000]. In addition, the block along which India is sliding along its eastern boundary is not stable Eurasia, but rather the Sundaland block [Simons *et al.*, 1999; Michel *et al.*, 2001]. Taking this into account, the relative motion expected between India and Sundaland on the Myanmar boundary reduces to 43 mm/yr at N7°E. It is generally assumed that most of this motion is accommodated by the active right-lateral strike-slip Sagaing fault system, running approximately north-south through Myanmar (Figure 1).

As a first step toward mapping the distribution of the India-Eurasia or India-Sunda motions within the Eastern Himalayan Syntaxis area, we have installed and measured twice (1998 and 2000) a high-precision GPS network in Myanmar.

2. Geodynamic Setting

[3] The Myanmar mountain belts and basins record the recent and active slip of India along the western margin of Indochina (or Sundaland). Three main tectonic provinces, all elongated N-S and extending from the East Himalayan Syntaxis in the north to the Andaman Sea into the south, can be identified (Figure 1).

[4] 1. The Arakan Yoma belt (or Indo Myanmar belt) [Brunnschweiler, 1966] is an arcuate sedimentary belt mainly formed by Cenozoic rocks and cored by Triassic metamorphic basement [Socquet *et al.*, 2002]. It is classically considered as an active accretionary wedge linked to the eastward subduction of the Bengal basin oceanic crust [Acharyya, 1978; Bender, 1983; Nandy, 1986].

[5] 2. The Myanmar central basin (MCB), located immediately east of the Rakhine Belt, in the central Myanmar Lowlands, is a series of Cenozoic basins presently affected by an active inversion [Pivnik *et al.*, 1998]. These basins extend southward in the Andaman Sea and are classically

¹Ecole Normale Supérieure, CNRS, Paris, France.

²Institut Géographique National, Marne la Vallée, France.

³Now at Albert-Ludwigs-Universität, Freiburg, Germany.

⁴Institut für Geodäsie, Universität der Bundeswehr, Neubiberg, Germany.

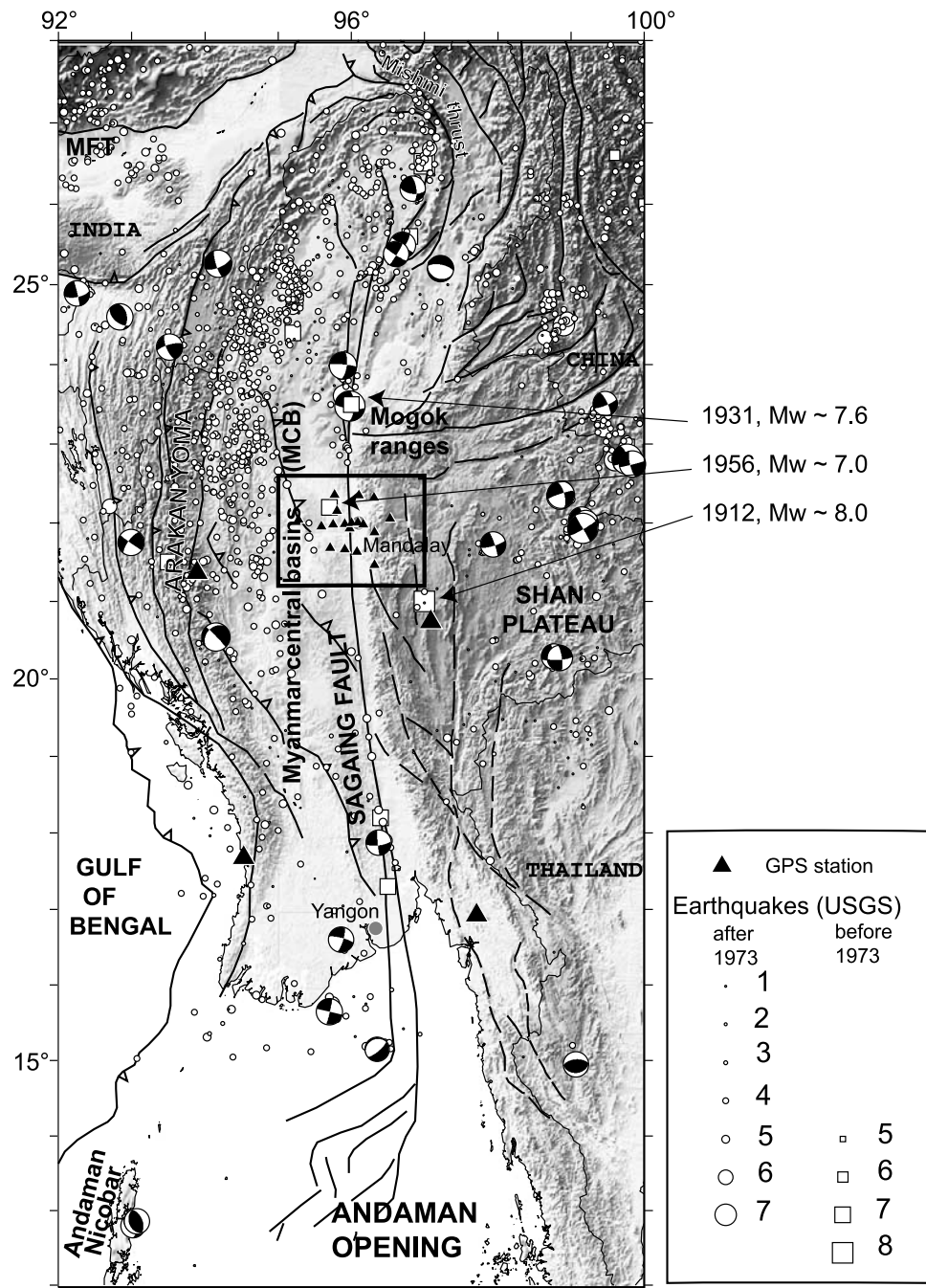


Figure 1. Myanmar tectonic setting. Earthquake locations are from the USGS catalog and depict recent (circles) and historical (squares) earthquakes. Focal mechanisms are from CMT [Dziewonski *et al.*, 1981, 1996]. Solid triangles show locations of GPS stations.

considered as a couple of forearc/back arc basins for the Bengal subduction system.

[6] 3. The Shan Plateau, with an average elevation of 1000 m is the natural eastward boundary for the MCB and the major topographic relief of the Sino-Myanmar ranges [Mitchell, 1989; Rangin *et al.*, 1999]. It is considered as the western edge of the rigid Sundaland block. Actually this topographic boundary trends NNW-SSE from latitude of Yangon to Mandalay, then swings NE-SW from the Mogok Range to western Yunnan (China) and finally trends north to connect with eastern Tibet. The Sagaing fault, classically

considered as the tectonic boundary between the Shan Plateau and the MCB, is actually crosscutting the MCB with a regular N-S trend [Bertrand *et al.*, 2001].

[7] The Indo-Myanmar-Sino Ranges terminate northward in the Eastern Himalayan Syntaxis (EHS) [Mitchell, 1993], one of the most active tectonic zones on earth. The EHS is characterized by a 180° rotation of the regional active structures. Here the actively deformed northern Arakan Yoma subducts northward below the Eastern Himalaya Main Boundary Thrust, meanwhile the Sino Myanmar Ranges connect northward with eastern Tibet, around the

EHS. Between both, the MCB is considerably deformed in the core of this structural bend. In the south, the Arakan Yoma belt extends southward to the Andaman and Nicobar archipelago, while in the east the Sino Myanmar Ranges extend into peninsular Malaysia. The Andaman Sea appears as the direct offshore continuation of the MCB.

[8] Most of the seismic activity defines a platelet bordered westward by the Andaman trench and eastward by the edge of the Shan Plateau, the Shan Scarp (Figure 1). In the field, recent tectonic activity is visible across this platelet. However, seismicity is concentrated along the eastern flank of the Arakan Yoma belt, along the Sagaing fault and along the northern Shan Plateau, suggesting that motion is accommodated on localized structures rather than being distributed throughout. Focal mechanisms of major superficial earthquakes (<30 km depth) and field work observations of the major active faults indicate that dextral strike slip is distributed on both sides of the central lowlands, in the eastern foothills of the Arakan Yoma and the western foothills of the Shan scarp (Figure 1). The central lowlands where the Myanmar central basins were developed during the Cenozoic, are presently affected by compression and basin inversion [Rangin *et al.*, 1999], but seismicity remains scarce in central Myanmar (20°N–23°N).

3. Tectonic Description of the Sagaing Fault Zone

[9] The central 700 km of the Sagaing fault is remarkably linear (17°N–23°N). The fault has a clearly defined morphology between Swebo and Mandalay (22°N), but is more difficult to trace southward on satellite images and in the field (Figure 2). The fault branches in various splays north of Swebo (22.5°N) and terminates in the Jade Mine belt into a compressive 200-km-wide horse tail structure. Further north, this fault connects with the Mishmi Thrust, the western termination of the Himalayan Main Central Thrust. Southward, the fault terminates as a horse tail extensional system connecting to the Andaman spreading center [Rangin *et al.*, 2001]. In its central part, the trace of the fault is distinct from the trace of the faults observed along the foothills of the Shan Scarp [Bertrand, 2000].

[10] The Sagaing fault crosscuts series of complex structures that affect both the edge of the Shan Plateau and the central Myanmar basins (Figure 2). The N160° trending edge of the Shan Plateau connects with the Sagaing fault trace at the latitude of Swebo. To the south, the edge of the plateau is framed by series of N160° vertical or slightly west verging reverse faults connecting to N50° trending north facing normal faults [Bertrand *et al.*, 2000]. This dog-leg shape structure outlines the Shan Scarp fault. This trans-tensile fault dies out progressively southward and delineates a large depression. North of Swebo, similar trans-tensile geometry was mapped, west of the Sagaing fault (Figure 2). The nature of the outcrops (gneisses and Mesozoic/Paleozoic sediments associated with volcano-plutonic rocks) indicates that the edge of the Shan Plateau extends into this area. These two segments of the Shan Plateau border (north and south of Swebo) are slightly offset by the Sagaing fault, indicating that the Sagaing fault is very recent. On the contrary the Shan Scarp fault is rather linear, and dies out southward at the junction with the Three Pagodas fault. South of Mandalay the Shan Scarp fault foothills are formed

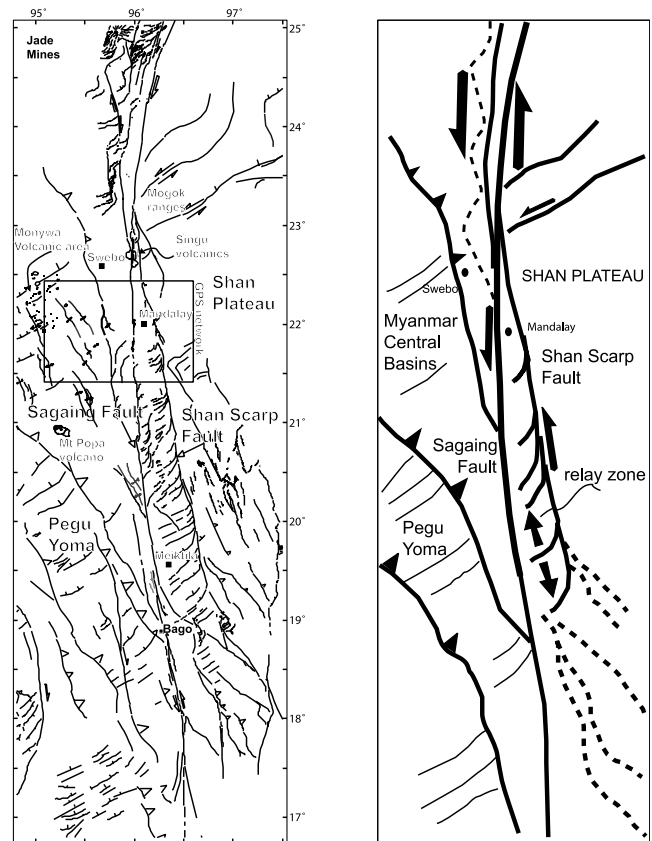


Figure 2. (left) Landsat TM and SPOT image interpretation of the Sagaing fault and Shan Scarp fault zone and (right) simplified tectonic interpretation.

by faulted Cenozoic gneissic domes. Metamorphism was dated between 25 and 14 Ma, and pervasive N160°E trending lineations are interpreted as steady state stretching along the Shan Scarp fault [Bertrand *et al.*, 1998, 2001].

[11] The Sagaing fault has been interpreted as being a plate boundary between India and Sundaland [Le Dain *et al.*, 1984; Guzman-Speziale and Ni, 1996]. However, some authors have pointed out that a significant part of the relative motion between the two plates could be accommodated by other tectonic structures [Maung, 1987; Holt *et al.*, 1991]. Active deformation observed in the Myanmar central basins [Pivnik *et al.*, 1998], indicates part of the India/Eurasia motion is absorbed along the N140°E trending wrench faults present there. NE and SW of Swebo, very recent volcanic vents were emplaced along tension gashes and normal faults perpendicular to these thrusts. The Mont Popa (21°N) and Monywa (22, 5°N) volcanism is probably emplaced in the same tectonic setting. In addition, large and continuous N-S trending dextral strike-slip faults affect the Arakan Yoma Wedge. These faults are associated with discrete pull-apart basins in the core of the range. The most significant one is the Manipur Valley in India [Ni *et al.*, 1989]. These faults connect to the south on N140° trending thrusts present in the southern part of the Arakan Yoma. Active dextral motion was also evidenced offshore along the front of the Arakan Yoma Wedge in southern Myanmar [Nielsen *et al.*, 2001]. Multibeam echo sounder bathymetry

combined with shallow penetration seismic lines collected during the “Andaman Cruise” [Chamot-Rooke *et al.*, 2001a] reveal that the motion along this hyper oblique subduction is partitioned between minor N140° trending shortening zones and dominant N20° to N30°E dextral transform faults. At the regional scale, this plate boundary can be interpreted as a dextral transform shear zone making the link between two major accretionary wedges, the Andaman-Nicobar wedge in the south and the Indo-Burmese wedge in the north.

[12] Consequently, seismological and geological information indicate the Sagaing fault is located in the central part of a large shear band formed by the Shan scarp and the associated folds into the east, and active strike slip faulting located along the eastern flank of the Arakan Yoma into the west. In this shear band the inverted Myanmar central basins are characterized by SW or NE verging thrusts and NE trending normal faults. The Pegu Yoma anticline is one of several active en echelon folds. These observations suggest India/Eurasia dextral strike-slip motion is distributed across western Myanmar from the Arakan Yoma in the west, to the edge of the Shan Plateau into the east. GPS results presented here allow estimation of the amount of strain absorbed along the major faults and folds in this wide shear band.

4. GPS Network

[13] We installed a GPS network in 1997 in order to quantify the deformation in Myanmar. A large-scale rectangle of four points was designed to integrate all the deformation between the Main Boundary Thrust on the west side and the Sunda block on the east side, 300 km away. A more local network aimed at assessing the type and the amount of deformation accommodated by the Sagaing fault was also installed. This local network consists in three transects across the Sagaing fault at the latitude of Mandalay. One long transect (10 points, 140 km length) samples the deformation between the two north points of the large-scale network. Two shorter transects (4 points, 70 km length each) sample the deformation 35 km north and south of the main transect.

[14] The markers are 12 cm thread marks made of brass and copper. They are fixed in rock using a special stone-metal adhesive. The top of the marker is designed in the form of a screw thread protected by a removable cap. During the occupation of a site, the cap is removed and the GPS antenna is screwed on top of the marker, by means of a threaded adapter, which enables the antenna to be attached directly to the monument. In this way, antennas can be relocated with an accuracy of ~ 0.1 – 0.2 mm, so that eccentricity errors are not a concern. Whenever possible, the markers were sealed in hard bedrock outcrops. Unfortunately, in some areas around Mandalay (mostly on the western side of the fault), bedrock is scarce or absent. In such situations where bedrock could not be found, concrete benchmarks were built (1 m³, 1 m deep, reinforced and anchored at 2 m depth by iron rods) and the marker was sealed on top of the benchmark.

[15] The site locations were chosen so that final transects are as close as possible to straight lines running perpendicular to the fault. The interval between points ranges from

1 to 15 km and is smaller when closer to the fault in order to increase spatial definition in this area. The end points of the longest transect are 70 km away on each side of the fault, and 35 km away for the southern and northern transects. This distance of 70 km (and a fortiori 35 km) is not really far enough to be isolated from long-term viscoelastic effects, if they are present. However, the issue of viscoelastic effects is more an issue of time than space. The only significant events that might cause viscoelastic effects in the area nowadays are three historical earthquakes documented in USGS catalog (Figure 1): (1) 1912, $M_w \sim 8.0$, ~ 200 km SE of Mandalay, (2) 1934, $M_w \sim 7.6$, ~ 200 km N of Mandalay, and (3) 1956, $M_w \sim 7.0$, in the Mandalay area.

[16] Using standard exponential decays, with relaxation times around one year, residual motion 50 years later for $M_w \sim 7$ earthquakes is negligible. Only with much longer relaxation time (10 years), some significant motion can take place after many decades. In addition, based on observations of the similar-sized Landers and Hector Mine earthquakes in California, the total postseismic deformation for an $M_w \sim 7$ earthquake is likely to be < 10 cm. Therefore it is not likely that any of the three historical earthquakes produces more than 1 mm/yr of transient differential motions within the local network.

[17] Finally, 70 km from the fault plane is also not far enough away to detect 100% of the long-term motion. It will contain $\sim 90\%$ of the total amount for a 15 km locking depth. Nevertheless, the quantification of the deformation pattern in a 150-km-wide band around the fault by 10 points well spaced allows to estimate both the locking depth and the far field velocity by fitting an elastic model.

5. GPS Measurements and Data Processing

[18] The first GPS campaign was conducted during October 1998. The 22 sites were measured with five dual frequency receivers (Trimble SSE), equipped with standard Trimble SST antennas. The Mandalay area network was measured first, three sites being measured continuously (MDPG, KWEH, YWEN) for 12 days, while the remaining sites were measured two by two in single 24-hour sessions. The four sites belonging to the large-scale network (HPAA, LAUN MIND, TAUN) were measured separately during 5 continuous days, during 2 of which the MDPG station of the small-scale network was still in operation. Sixty-nine out of the 231 possible baselines were measured at least twice. The second GPS campaign was conducted during November 2000. This time, seven Ashtech Z-XII receivers equipped with choke-ring antennas were used. The three sites (MDPG, KWEH, YWEN) in the Mandalay area were measured continuously for 14 days, while the other local network sites were measured with four roving receivers in 24-hour sessions. The four large-scale network sites were measured in 5 days, while the three local continuous sites being still in operation. Because of the increased number of receivers, 105 baselines were measured at least twice.

[19] The solution presented here is computed using the GAMIT/GLOBK software [King and Bock, 1999; Herring, 1999]. The 24-hour measurement sessions are reduced to daily positions using the ionosphere-free combination and fixing the ambiguities to integer values. We used precise orbits from the International GPS Service for Geodynamics

(IGS) [Beutler *et al.*, 1993]. We also used IGS tables for modeling of antenna phase center variations. We do not use externally determined meteorological data but rather use the data themselves to estimate tropospheric delay parameters (one every 3 hours). For both campaigns, average horizontal baseline repeatabilities (scatter about the root mean square value) are of the order of a few millimeters for most local baselines (<150 km).

[20] Baselines involving only IGS stations have equivalent repeatabilities for both 1998 and 2000 measurement epochs (3–5 mm for 2000-km-long baselines), while local repeatabilities improve from 3.0–4.6 mm in 1998 to 1.2–3.3 mm in 2000. This amelioration is characteristic as it is also shown by the three most measured local baselines (MDPG, KWEH, YWEN). This can be explained by the systematic use of choke-ring antennas and the increased number of simultaneous measurements within the local network in 2000.

[21] Solutions in a consistent reference frame were obtained at both epochs by including data from 12 permanent IGS network stations available in the area (COCO, GUAM, IISC, KARR, KUNM, LHAS, SHAO, TIDB, TSKB, WUHN, XIAN, YAR1) [Neilan, 1995]. These daily data were combined with the daily GAMIT solutions into a loose system using Helmert type transformations in which translation, rotation, scale and Earth orientation parameters (polar motion and rotation) are estimated. The reference frame is then defined by minimizing, in the least squares sense, the departure from a priori values based on the International Terrestrial Reference Frame (ITRF) 2000 [Altamimi *et al.*, 2002], of the positions and velocities of a set of well determined stations (GUAM, IISC, KARR, KUNM, LHAS, SHAO, TIDB, TSKB, WUHN, XIAN, YAR1). The misfit to those fiducial stations is 1.7 mm for positions and 1.1 mm/yr for velocities. Such small values indicate that local velocities are consistently computed in a stable reference frame.

[22] The true uncertainty is function of the reference frame; the uncertainty of relative velocities within the Mandalay network is significantly smaller than the uncertainty of the velocities with respect to a global or regional frame. Contrary to 2000, in 1998, the local Mandalay network and the regional Myanmar network were measured successively and not simultaneously (apart from 2 days at one local station). This implies that for 1998, the tie of the local network to the regional one relies on very long baselines to far away IGS stations.

[23] Therefore, when local network internal deformation uncertainty is well represented by short baselines repeatabilities (i.e., 1–2 mm), the overall motion of the local area with respect to the regional frame is affected by very long baselines uncertainty (i.e., 5–7 mm implying 3–4 mm/yr). In summary, the internal relative deformation within both networks (local Mandalay network and regional Myanmar network) is known with a better accuracy (<2 mm/yr) than the motion of Mandalay area with respect to regional (Sundaland or Myanmar platelet) frame (~3–4 mm/yr).

6. Data Analysis

[24] Additional data from regional campaigns in South-east Asia (GEODYSSSEA) [Simons *et al.*, 1999; Michel *et*

al., 2001] are also used to improve site positions and define a regional reference frame. GEODYSSSEA campaigns were conducted in 94, 96, 98, and 2000, and include more than 60 stations spanning whole South East Asia. Twelve of these sites are located within the so-called “Sundaland platelet” (BALI, BUTU, BAKO, BATU, TANJ, BLKP, TABA, BRUN, KUAL, PHUK, CHON, NONN), to which the two easternmost Myanmar sites (HPAA, TAUN) can be added. These 14 sites velocities depict the rotation of a rigid block, the Sundaland block. We can determine the position and angular velocity of the Sundaland rotation pole that best fits the observed Sundaland stations velocities in ITRF 2000. This gives an absolute pole at $59 \pm 4^\circ\text{S}$, $81 \pm 3^\circ\text{E}$ with an angular rotation rate of $0.303 \pm 0/01^\circ/\text{Myr}$. This determination is slightly different from the pole derived from the GEODYSSSEA combined solution (56°S , 77°E , $0.339^\circ/\text{Myr}$) [Michel *et al.*, 2001], but within the uncertainties.

[25] The motion relative to neighboring plates (Eurasia or Australia) can be obtained by subtracting the absolute pole of these plates in the same reference frame. ITRF is supposedly aligned with NNR-NUVEL-1A. Thus subtracting the absolute Eurasian or Australian pole given by DeMets *et al.* [1994] to our ITRF 2000 Sundaland pole gives a relative pole describing the relative motion between pairs of plates. The result is within the range of possible poles obtained by combining GPS data with slip vectors data at Sunda trenches [Chamot-Rooke and Le Pichon, 1999]. The small difference can be attributed to the use of ITRF2000 instead of ITRF97, additional data on existing points since 1998, and the introduction of new stations in the processing, in particular the incorporation of Myanmar data. In this Sunda reference frame, eastern Myanmar sites (TAUN and HPAA) exhibit small residual velocities, indicating they are located within stable Sundaland (Figure 3 and Table 1).

[26] Since we use only one site on the India plate (IISC) it is not possible to estimate the position of a rigid rotation pole and an angular velocity for this plate. Nevertheless, and as noted by previous authors [Chen *et al.*, 2000; Shen *et al.*, 2000; Paul *et al.*, 2001], our solution also indicates a slower India plate than expected from geological models (Figure 3 and Table 2). Our determination of IISC velocity with respect to Eurasia is 41 mm/yr, which is 8 mm/yr smaller than the NUVEL-1A prediction, and 4 mm smaller than the latest geodetic determination [Paul *et al.*, 2001]. The velocity at IISC (35.9 ± 1 mm/yr) with respect to Eurasia determined by Wang *et al.* [2001] is slightly smaller than ours, but the reference frame is also slightly different. We use the NUVEL-1A Eurasia while they use their own determination based on the motion of 11 GPS stations. This GPS Eurasia moves a few millimeters north with respect to NUVEL-1A Eurasia at this longitude implying a decrease of the relative motion between India and Eurasia.

[27] Relative to Sundaland, Western Myanmar velocities indicate that the total amount of dextral strike-slip deformation across the Myanmar platelet ranges from slightly less than 30 mm/yr in the south (LAUN) to 25 mm/yr in central Myanmar (MIND) (Figure 3). Close analysis of transect velocities reveals that only two thirds of the deformation is accommodated on the Sagaing fault (slightly less than 20 mm/yr), with the remaining 10 mm/yr occur in

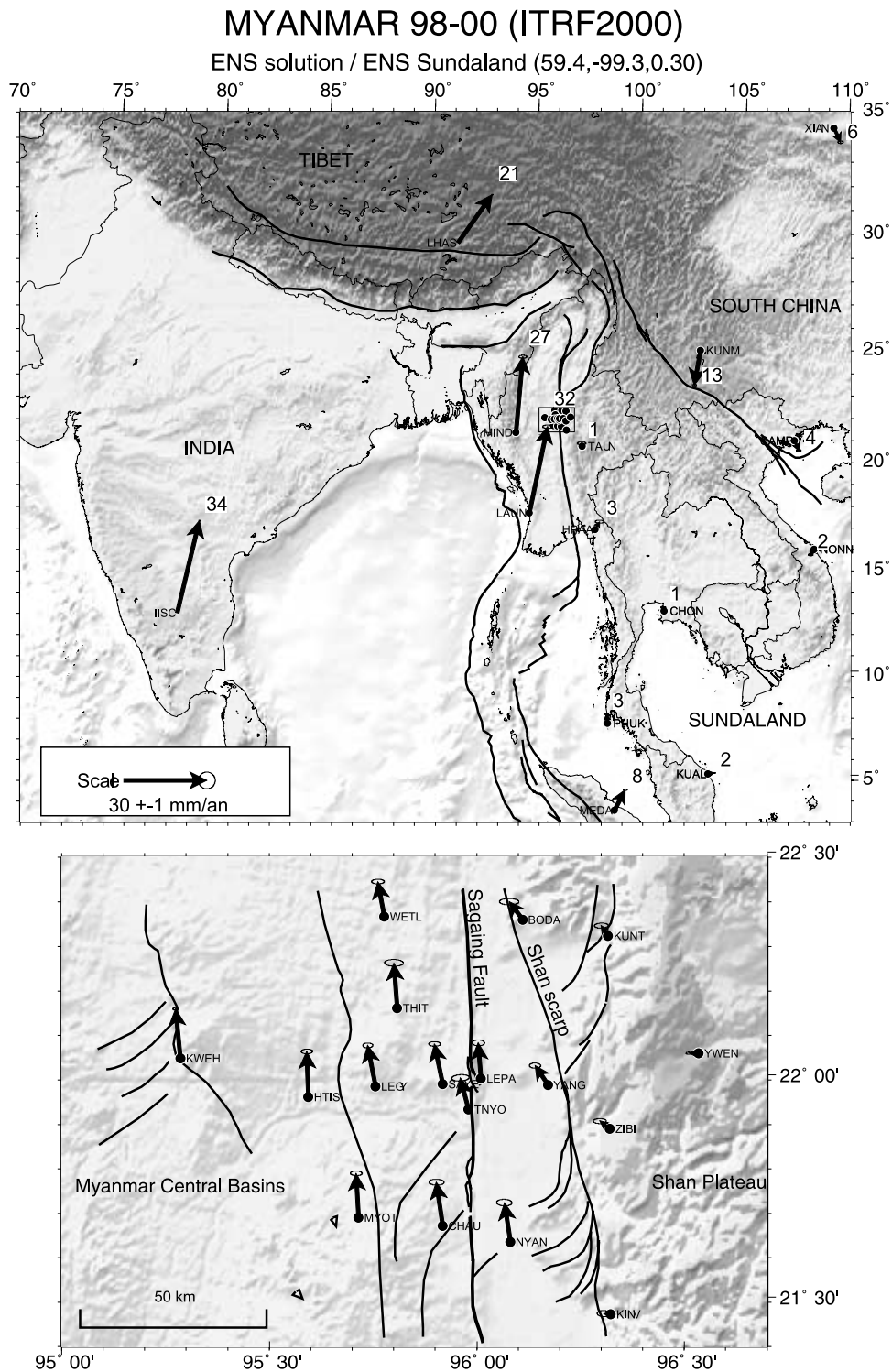


Figure 3. (top) Regional and Myanmar velocities in the Sundaland reference frame. (bottom) Mandalay area transect stations. Error ellipses show the 99% confidence level of formal uncertainties given in Table 1.

the Arakan Yoma belt and in the Burma trench itself west of the fault [Nielsen *et al.*, 2001]. With the exception of MDPG (not shown on figure) intermediate site velocities show the typical signature of a locked fault with accumulation of elastic deformation around the fault trace (Figure 3 and Table 1). It should be noted that the southernmost sites

exhibit slightly higher velocities than the sites 60 km northward.

[28] Using each site velocity and distance to the center of the network, one can construct the normal equations to estimate the constant bias term and the velocity gradient throughout the whole network, based on the formula of

Table 1. Myanmar Sites Velocities^a

Site	Longitude	Latitude	ITRF2000		Sundaland		E_{lon}	E_{lat}	Correlation	
			V_{lon}	V_{lat}	V_{lon}	V_{lat}				
<i>Myanmar Large-Scale Network</i>										
HPAA	97.715	16.938	34.11	-2.25	1.59	2.77	0.53	0.18	-0.005	
LAUN	94.537	17.692	39.28	27.15	6.59	31.25	0.60	0.20	-0.005	
TAUN	97.094	20.750	32.66	-3.79	-0.29	1.05	0.52	0.17	-0.003	
MIND	93.897	21.383	35.55	23.43	2.46	27.35	0.49	0.18	0.007	
<i>Mandalay South Transect</i>										
KINV	96.323	21.473	30.56	-4.46	-2.47	0.16	0.80	0.37	-0.089	
NYAN	96.081	21.636	30.88	9.65	-2.17	14.20	0.91	0.39	-0.066	
CHAU	95.919	21.672	30.68	11.30	-2.38	15.80	0.90	0.35	-0.056	
MYOT	95.716	21.691	32.16	11.54	-0.91	15.98	0.70	0.28	-0.027	
<i>Mandalay Central Transect</i>										
ZIBI	96.321	21.890	29.42	-1.76	-3.65	2.86	0.79	0.29	0.003	
TNYO	95.981	21.934	30.04	6.91	-3.04	11.43	1.05	0.39	-0.158	
HTIS	95.595	21.962	32.46	12.08	-0.63	16.49	0.68	0.28	0.021	
LEGY	95.757	21.986	30.18	10.34	-2.91	14.80	0.60	0.29	0.023	
YANG	96.172	21.989	28.37	2.44	-4.71	7.02	0.68	0.31	-0.040	
SAYE	95.919	21.991	30.01	10.04	-3.08	14.54	0.69	0.28	-0.013	
LEPA	96.011	22.003	32.04	8.46	-1.05	12.99	0.74	0.35	-0.025	
MDPG ^b	96.097	22.009	9.54	2.10	-23.54	6.65	0.31	0.12	-0.010	
KWEH	95.286	22.049	31.35	13.56	-1.76	17.88	0.34	0.13	0.034	
YWEN	96.535	22.060	29.54	-4.61	-3.53	0.07	0.34	0.13	0.014	
<i>Mandalay North Transect</i>										
THIT	95.809	22.162	31.86	11.86	-1.24	16.33	1.12	0.40	-0.044	
KUNT	96.317	22.324	30.60	-0.96	-2.50	3.66	0.83	0.30	0.078	
BODA	96.111	22.360	28.20	1.96	-4.91	6.52	1.17	0.38	-0.012	
WETL	95.778	22.367	30.73	8.20	-2.39	12.66	0.75	0.28	0.017	

^aVelocities are in units of mm/yr.

^bRejected from the solution. The antenna used at Mandalay throughout the whole campaign in 2000 later revealed a constant offset of around 2–3 cm. The cause of this offset remains unknown but is confirmed by calibrations.

Feigl *et al.* [1990]. Then the velocity gradient is used to form the average strain and rotation rates within the network. This method is used to compute strain and rotation rates in different areas within the network (Figures 4a and 4b). Internal strain and rotation rates are not affected by reference frame uncertainties.

[29] The triangle between South India (IISC) and the two West Myanmar points (Figure 4a, top left) yields 10 nstrain/yr oriented N21° and -11 nstrain/yr on the perpendicular axis. This corresponds to pure right-lateral strike-slip motion, almost perfectly aligned with the Andaman Trough. Obviously the rate does not mean much because the amount of shear depends of the size of the triangle and strain is probably concentrated in a very small part of it. Nevertheless, the direction of the main strain axis and the fact that it corresponds to strike-slip deformation will not change whatever Indian point we use to define the triangle, as long as the plate is rigid.

[30] The large-scale Myanmar rectangle (MIND, TAUN, HPAA, LAUN) (Figure 4a, top center) and the polygon including the local network (Figure 4a, top right) give respectively 34, -65 nstrain/yr and 66, -118 nstrain/yr with the same orientation at N43°. This corresponds to right-lateral strike-slip motions aligned on the Sagaing fault strike, with a small amount of NE-SW trending compression. Details in a Delauney triangulation of the local network (Figure 4a, bottom) reveal the same right-lateral strike-slip pattern superimposed with oblique compression. Rotations within the same subareas (Figure 4b) reveal small (0.4°/Myr) anticlockwise rotation of the Myanmar platelet

with respect to India (Figure 4b, top left), and clockwise rotations everywhere else across the fault. The fact that strains and rotations rates are higher on the east side of the fault than on the west side (Figure 4a, bottom and Figure 4b, bottom), indicate that the maximum shear zone is not centered on the fault trace itself, but rather shifted to the east.

[31] Figure 5 depicts the site's fault-parallel velocity components plotted against their distance to the fault trace. The data nicely follow an arctangent curve, and we thus adopt the model of [Savage and Burford, 1973] for the elastic two-dimensional deformation of an infinite strike-slip fault. The model is derived from the screw dislocation theory and assumes locking on the fault to depth D and slip by a constant amount below. We invert simultaneously for the depth of locking, the velocity and the position of the fault. The best fit elastic model parameter corresponds to a fault plane locked at approximately 15 km depth, with a far

Table 2. Bangalore (IISC) GPS Station Velocity^a

	V_{lon}	V_{lat}	E_{lon}	E_{lat}	Correlation
ITRF2000	40.7	33.9	1.3	0.2	
This solution (ITRF2000)	40.13	34.31	0.09	0.05	0.080
NNR-NUVEL-1A (Eurasia)	16.8	43.8			
Paul <i>et al.</i> [2001] (Eurasia)	16.6	40.4			
ITRF2000 (Eurasia)	17.8	36.7	1.3	0.2	
This solution (Eurasia)	17.27	37.12	0.09	0.05	0.080
This solution (Sundaland)	8.02	33.37	0.09	0.05	0.080

^aVelocities are in units of mm/yr.

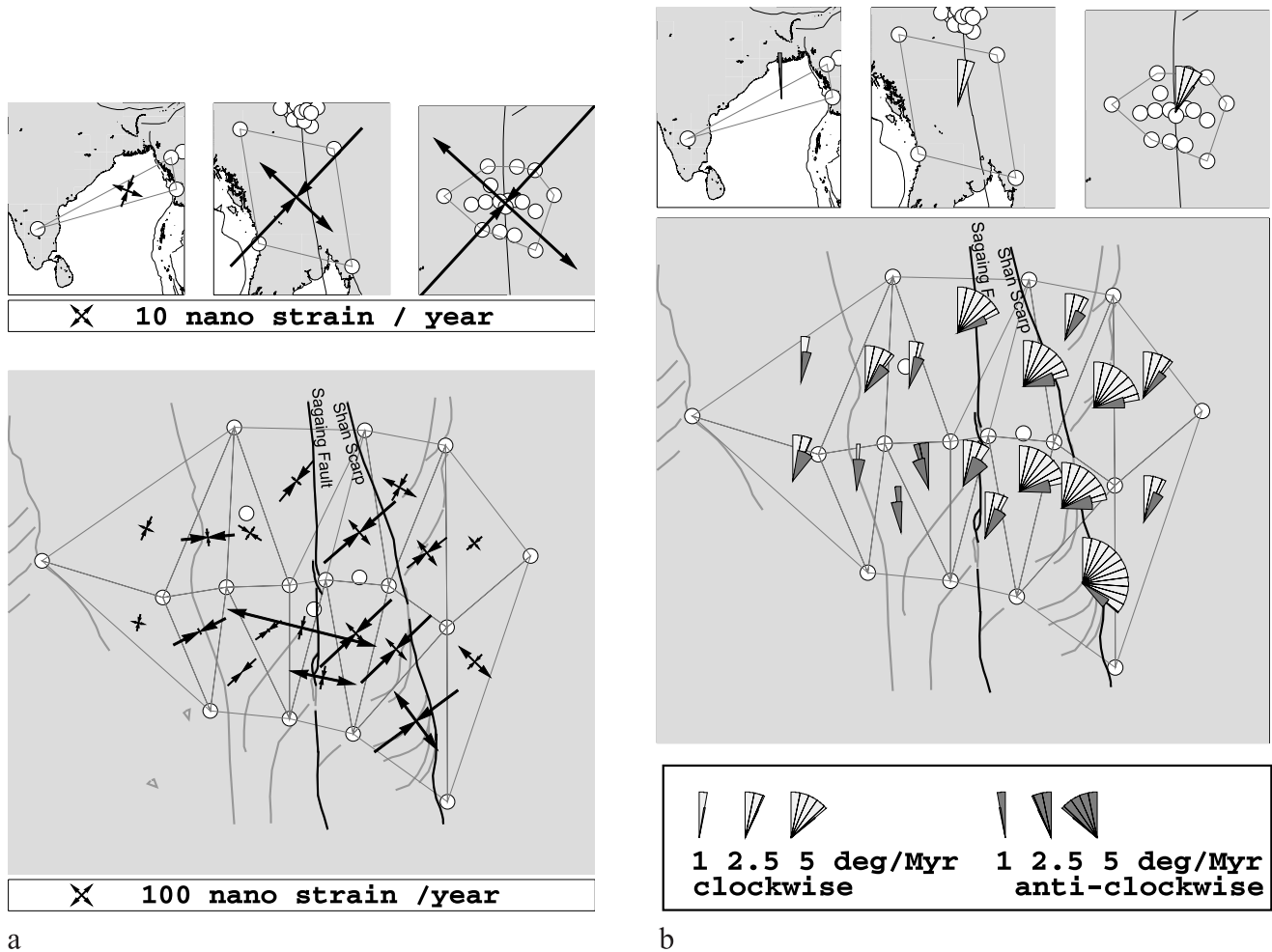


Figure 4. (a) Strain rates and (b) rotation rates in the Myanmar network. Vectors are aligned with strain tensor principal axis directions. Inward pointing arrows depict compression. White color wedges depict clockwise block rotations and gray color wedges depict anticlockwise rotations.

field velocity of ~ 18 mm/yr. We also find that the best fit profile is shifted 17 km east of the fault. In other words, the location of maximum shear strain is not centered on the surface geological fault trace, but rather between the Sagaing fault and the Shan scarp. Whether this fact allows discriminating between active structures or whether it indicates a more complex 3D geometry remains debatable. It is clear that the 2D simplistic model does not take into account fault plane dipping or nonconstant velocity along the fault plane or distinct rheologies on each side of fault system. The interseismic deformation only depends on the location of the dislocation line at depth and a simple explanation for an offset between this dislocation line and the surface trace of the fault would be to consider a shallow-dipping fault (40°). This option would suggest a connection with the Shan Scarp at depth. However, the Sagaing fault is a pure strike-slip fault without any related topography, implying that the slip must be horizontal even though the fault is dipping. Alternatively, that offset could reflect the possibility that another parallel fault (the Shan Scarp) is in fact more active.

[32] Finally, a careful along-strike analysis of velocities reveals that there is a tendency for northward decreasing

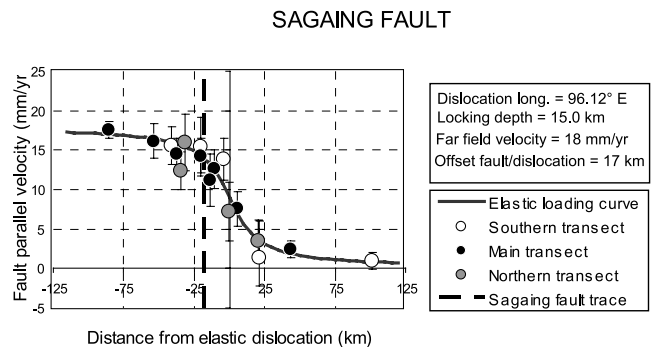


Figure 5. Elastic loading across Sagaing fault. Fault parallel velocity component in mm/yr (dots) as a function of distance to fault trace. Gray, solid, and open circles represent northern, central, and southern transect fault-parallel velocities, respectively. The solid curved line shows the best fit profile obtained for a locking depth of 15 km. Vertical dashed line shows location of the Sagaing fault, 17 km west of the elastic dislocation.

velocities. In addition, south transect points show a steeper profile than the north transect points (Figure 5). This suggests that the locking depth is shallower in the south than in the north. This can also be discussed in term of modification of the fault velocity and/or fault plane geometry (bending and depth) with latitude, and/or non symmetrical rheology. However, since the effect is very slim (± 1 mm/yr), the possibility that transect velocities might be affected by very long term postseismic effects following M_w 7 Mandalay earthquake can not be rejected without careful analysis. Therefore this spatial variation will be investigated in more detail in the future with additional measurements, further away from the fault, higher and lower in latitude.

7. Tectonic Interpretation

[33] At the scale of the Burma platelet GPS data confirm that the Sagaing/Shan Scarp fault system is the main strike-slip fault zone along which 60% (~ 20 mm/yr) of the India/Sundaland motion is presently absorbed. This instantaneous rate on the Sagaing fault is comparable to the mean motion for the last 300,000 yrs, which has been estimated between 10 and 23 mm/yr from the offset of the Quaternary Singu volcano (Figure 2) in the Swebo area [Bertrand *et al.*, 1998].

[34] GPS measurements further indicate that an amount over 10 mm/yr of dextral motion shall be absorbed west of the Sagaing fault system. This amount depends of the total strike-slip motion estimated between India and rigid Sundaland, which is still poorly known as we dispose of only one site (IISC) on the Indian plate. However, we can propose that if 60% of the India/Sundaland oblique relative motion is absorbed along the Sagaing/Shan Scarp fault system, the remaining 40% shall be absorbed in the Burma platelet toward the west. Potential structures for localization of this deformation are the active wrench faults that affect both the central basins and the Arakan Yoma belt. However, similar wrenching characterizes the frontal Arakan Yoma wedge in the Andaman trench [Chamot-Rooke *et al.*, 2001b; Nielsen *et al.*, 2001].

[35] Active deformation is outlined by wrenching and inversion of the central basins and partly along the eastern flank of the Arakan Yoma east of Mindat GPS station. Folding and thrusting in the Basins is very recent and probably active as indicated by the deformation of the Wurm erosion surfaces and the folding of the Irrawaddy formation of Plio-Quaternary age [Pivnik *et al.*, 1998]. N140°E trending “en echelon” folds and thrusts affect these basins and numerous N50°E trending active normal faults are intruded by recent and active volcanism. This is the case in the Monywa area where large diatremes are aligned along these faults. A similar setting can be observed southward in the mount Popa area (Figure 2). The slight northward decrease of the total amount of deformation observed in the GPS data, might account for this diffuse basin shortening along NW-SE thrusts and folds. Significant strike-slip deformation has also to be absorbed west of Mindat GPS station along the Arakan trench or along N-S trending faults affecting the Arakan Yoma fold-and-thrust belt.

[36] The local network installed across the Sagaing/Shan Scarp fault system, in the Mandalay area, provides infor-

mation on how strain is partitioned on distinct structures identified in this region. The Sagaing fault trends N-S in the Mandalay area but swings N10°E northward and N170°E southward, providing a slight arc shape to this fault trace. In the field, the Sagaing fault appears mainly subvertical with small relay zones (Idawgyii and Yega lakes pull-apart close to Sagaing City). The linearity of the fault is generally good and its trace is easy to map both north of the city of Sagaing and south of Bago. Only the central segment of this fault, south of Mandalay, is rather difficult to identify both in the field and on satellite images. Therefore it is difficult to discriminate between the different hypothesis (dipping fault or activity of the Shan Scarp fault) in this area. GPS measurement might help us to discriminate, in particular by analyzing velocities differences of the points located between the two faults. However, the different models yield millimetric differences; therefore it seems untimely to interpret our data set at this level of precision.

8. Conclusion

[37] Two GPS campaigns 2 years apart are a strict minimum to assess the deformation pattern with a reasonable precision. This is acceptable when field measurements are realized in good conditions: enough redundancy to allow rejection of errors, 24-hour sessions to average different troposphere conditions, continuous sites throughout the campaigns to maintain a stable scale, identical antennas to cancel phase center offsets, threaded markers to avoid centering errors, and data processing done with state-of-the art technique (software, IGS orbits, fiducial stations, ITRF mapping). However difficult it may be to determine GPS measurement’s real precision (vs. formal uncertainties), our results have a remarkable consistency with very small scatter and residuals with respect to a simple model, especially within the Mandalay local network. The deformation pattern in the area simply reflects sliding of rigid India against rigid Sundaland along the almost pure strike-slip Sagaing fault, presently locked. In addition to slip on the Sagaing fault, a significant amount (>10 mm/yr) of India-Sundaland motion is absorbed by strike-slip deformation west of the fault, possibly in the central Myanmar basins. Strike-slip motion onto the Sagaing fault amounts to 20 mm/yr, which is considerably less than previous estimates [Le Dain *et al.*, 1984; DeMets *et al.*, 1994], but which matches well a reduced angular velocity of India [Paul *et al.*, 2001], together with the accompanying motion of Sundaland against Eurasia [Chamot-Rooke and Le Pichon, 1999; Michel *et al.*, 2001]. The offset between the Sagaing geologic fault trace and the zone of maximum shear can be discussed in terms of activity of the Shan Scarp in central Myanmar, lateral variations of crust rheology and thickness, dip of the fault plane or a combined effect of these phenomena. Improved spatial coverage, in particular in the central basins west of the fault and further south of Mandalay will be required to better resolve the details of the deformation pattern.

[38] **Acknowledgments.** The Myanmar program was initiated in the framework of the GEODYSSSEA project under contract C11*-CT93-0337 between the European Commission and the GFZ in Germany. The bulk of this work has been sponsored by TMEP (GIAC project), and partially funded by INSU Programme National des Risques Naturels (PNRN).

References

- Acharyya, S. K., Mobile belts of the Burma-Malaya and the Himalaya and their implications on Gondwana and Cathaysia/Lauresia continent configurations, paper presented at 3rd Regional Congress on Geology, Mineral and Energy Resources of Southeast Asia, 1978.
- Altamimi, Z., P. Sillard, and C. Boucher, ITRF2000: A new release of the International Terrestrial Reference Frame for earth science applications, *J. Geophys. Res.*, 107(B10), 2214, doi:10.1029/2001JB000561, 2002.
- Bender, F., *Geology of Burma, Beitr. Reg. Geol. Erde*, vol. 16, Gebr. Borntraeger, Stuttgart, Germany, 1983.
- Bertrand, G., C. Rangin, R. C. Maury, H. M. Htun, H. Bellon, and J. P. Guillaud, The Singu basalts (Myanmar): New constraints for the amount of recent offset on the Sagaing Fault, *C. R. Acad. Sci., Ser. I*, 327(7), 479–484, 1998.
- Bertrand, G., C. Rangin, H. Maluski, and H. Bellon, Diachronous cooling along the Mogok Metamorphic Belt (Shan scarp, Myanmar): The trace of the northward migration of the Indian syntaxis, *J. Asian Earth Sci.*, 19, 649–659, 2001.
- Beutler, G., J. Kouba, and T. Springer, Combining the orbits of the IGS processing centers, in *Proceedings of the IGS Analysis Center Workshop*, edited by J. Kuba, pp. 20–56, Geod. Surv. of Can., Geomatics Can., Nat. Resour. Can., Ottawa, Ontario, 1993.
- Brunnschweiler, R. O., On the geology of Indo-Burman Range, (Arakan coast and Yoma, China Hills, Naga Hills), *J. Geol. Soc. Aust.*, 13, 137–194, 1966.
- Chamot-Rooke, N., and X. Le Pichon, GPS determined eastward Sundaland motion with respect to Eurasia confirmed by earthquake slip vectors at Sunda and Philippine trenches, *Earth Planet. Sci. Lett.*, 173, 439–455, 1999.
- Chamot-Rooke, N., C. Rangin, C. Nielsen, E. Bourdon, Min Han, Tin Tun Aung, Kyaw Htin, Min Swe, F. Farcy, and D. Tsang Hin Sun, Recent tectonics in the Bengal region: Preliminary results of the Andaman 2000 cruise (Andaman Basin, Burma front and northern Ninety East Ridge), *Geophys. Res. Abstr.* [CD-ROM], 3, 742, 2001a.
- Chamot-Rooke, N., C. Rangin, and C. Nielsen, Timing and kinematics of Andaman basin opening, *Eos Trans. AGU*, 82(20), Spring Meet. Suppl., Abstract T42B-08, 2001b.
- Chen, Z., B. C. Burchfield, Y. Liu, R. W. King, L. H. Royden, W. Tang, E. Wang, J. Zhao, and X. Zhang, GPS measurements from eastern Tibet and their implications for India/Eurasia intercontinental deformation, *J. Geophys. Res.*, 105, 16,215–16,227, 2000.
- DeMets, C., R. G. Gordon, D. F. Argus, and S. Stein, Effect of recent revisions to the geomagnetic reversal time scale on estimates of current plate motions, *Geophys. Res. Lett.*, 21, 2191–2194, 1994.
- Dziewonski, A. M., T.-A. Chou, and J. H. Woodhouse, Determination of earthquake source parameters from waveform data for studies of global and regional seismicity, *J. Geophys. Res.*, 86, 2825–2852, 1981.
- Dziewonski, A. M., G. Ekstrom, and M. P. Salagnik, Centroid-moment tensor solutions for July–September 1995, *Phys. Earth Planet. Inter.*, 97, 3–13, 1996.
- Feigl, K. L., R. W. King, and T. H. Jordan, Geodetic measurement of tectonic deformation in the Santa Maria fold and thrust belt, California, *J. Geophys. Res.*, 95, 2679–2699, 1990.
- Guzmanspeziale, M., and J. F. Ni, Seismicity and active tectonics of the western Sunda Arc, in *The Tectonic Evolution of Asia*, edited by A. Yin and T. M. Harrison, pp. 63–84, Cambridge Univ. Press, New York, 1996.
- Herring, T. A., Documentation for the GLOBK software version 5.01, Mass. Inst. of Technol., Cambridge, 1999.
- Holt, W. E., J. F. Ni, T. C. Wallace, and A. J. Haines, The active tectonics of the eastern Himalayan syntaxis and surrounding regions, *J. Geophys. Res.*, 96, 14,595–14,632, 1991.
- King, R. W., and Y. Bock, Documentation for the GAMIT GPS software analysis version 9.9, Mass. Inst. of Technol., Cambridge, 1999.
- Le Dain, A. Y., P. Tapponnier, and P. Molnar, Active faulting and tectonics of Burma and surrounding regions, *J. Geophys. Res.*, 89, 453–472, 1984.
- Maung, H., Transcurrent movements in the Burma-Andaman, *Geology*, 15, 911–912, 1987.
- Michel, G., et al., Crustal motion and block behavior in SE-Asia from GPS measurements, *Earth Planet. Sci. Lett.*, 187, 244–289, 2001.
- Mitchell, A. H. G., The Shan Plateau and western Burma: Mesozoic-Cenozoic plate boundaries and correlations with Tibet, in *Tectonic Evolution of the Tethyan Region, NATO ASI Ser., Ser. C*, edited by A. M. C. Sengör et al., pp. 567–583, Kluwer Acad., Norwell, Mass., 1989.
- Mitchell, A. H. G., Correlation of some tectonic belts in Thailand-Myanmar and China, *J. Geol. Soc.*, 150, 1089–1102, 1993.
- Nandy, D. R., Geology and tectonics of the Arakan Yoma, a reappraisal, *Bull. Geol. Soc. Malays.*, 20, 137–148, 1986.
- Neilan, R., The evolution of the IGS global network, current status, and future aspects, in *IGS Annual Report*, edited by J. F. Zumberge et al., *JPL Publ.*, 95-18, 25–34, 1995.
- Ni, J. F., et al., Accretionary tectonics of Burma and the three-dimensional geometry of the Burma subduction zone, *Geology*, 17, 68–71, 1989.
- Nielsen, C., C. Rangin, and N. Chamot-Rooke, Partitioning along the Indo-Burman wedge: Onshore and offshore constraints, paper presented at EUG XI Meeting, Eur. Union of Geosci., Strasbourg, France, 8–12 April 2001.
- Paul, J., et al., The motion and active deformation of India, *Geophys. Res. Lett.*, 28, 647–650, 2001.
- Pivnik, D. A., J. Nahm, R. S. Tucker, G. O. Smith, K. Nyein, M. Nyunt, and P. H. Maung, Polyphase deformation in a fore-arc/back-arc basin, Salin subbasin, Myanmar (Burma), *AAPG Bull.*, 82, 1837–1856, 1998.
- Rangin, C., Win Maw, San Lwin, Win Naing, C. Mouret, and G. Bertrand, Cenozoic pull-apart basins in central Myanmar: The trace of the path of India along the western margin of Sundaland, *Terra Abstr.*, 4, 59, 1999.
- Rangin, C., N. Chamot-Rooke, C. Nielsen, F. Farcy, Tsang Hin Sun, E. Bourdon, Tin Tun Aung, Min Han, Kyaw Htin, and Min Swe, Pull-apart basin history along the eastern Indian shear zone from Eocene to present, paper presented at EUG XI Meeting, Eur. Union of Geosci., Strasbourg, France, 8–12 April 2001.
- Savage, J. C., and R. O. Burford, Geodetic determination of relative plate motion in central California, *J. Geophys. Res.*, 78, 832–845, 1973.
- Shen, Z. K., C. K. Zhao, A. Yin, Y. X. Li, D. D. Jackson, P. Fang, and D. N. Dong, Contemporary crustal deformation in east Asia constrained by Global Positioning System measurements, *J. Geophys. Res.*, 105, 5721–5734, 2000.
- Simons, W. J. F., B. A. C. Ambrosius, R. Noomen, D. Angermann, P. Wilson, M. Becker, E. Reinhardt, A. Walpersdorf, and C. Vigny, Observing plate motions in S.E. Asia: Geodetic results of the GEODYSSSEA project, *Geophys. Res. Lett.*, 26, 2081–2084, 1999.
- Socquet, A., B. Goffé, M. Pubellier, and C. Rangin, Late Cretaceous to Eocene metamorphism of the internal zone of the Indo-Burma range (western Myanmar): Geodynamic implications, *C. R. Acad. Sci., Ser. 2*, 334(8), 573–580, 2002.
- Wang, Q., P. Z. Zhang, J. T. Freymueller, R. Bilham, K. M. Larson, X. Lai, X. Z. You, Z. J. Niu, J. C. Wu, Y. X. Li, J. N. Liu, Z. Q. Yang, and Q. Z. Chen, Present-day crustal deformation in China constrained by global positioning system measurements, *Science*, 294, 574–577, 2001.

M. Becker, Institut fuer Geodaesie, Universität der Bundeswehr, D-85577 Neubiberg, Germany. (matthias.becker@unibw-muenchen.de)

G. Bertrand, Geologisches Institut, Albert-Ludwigs-Universität, Albertstr. 23-B, D-79104 Freiburg, Germany. (bertrand@uni-freiburg.de)

M.-N. Bouin, LAREG, ENSG, 6 et 8, Av. Blaise Pascal, F-77455 Marne-La-Vallée, France. (bouin@ensg.ign.fr)

N. Chamot-Rooke, M. Pubellier, C. Rangin, A. Socquet, and C. Vigny, Ecole Normale Supérieure, Laboratoire de Géophysique, 24 Rue Lhomond, F-75231 Paris cedex 05, France. (rooke@geologie.ens.fr; pubellier@geologie.ens.fr; rangin@geologie.ens.fr; socquet@geologie.ens.fr; vigny@geophy.ens.fr)